

Lawrence Berkeley National Laboratory

Lawrence Berkeley National Laboratory

Title

MULTI-MAGNON LUMINESCENCE SIDEBANDS IN ANTIFERROMAGNETS

Permalink

<https://escholarship.org/uc/item/0bt4f4fv>

Author

Chiang, T.C

Publication Date

1977-12-01

Submitted to Physical Review Letters

UC-34

RECEIVED
LAWRENCE
BERKELEY LABORATORY

LBL-6992
Preprint C-1

MAR 8 1978

LIBRARY AND
DOCUMENTS SECTION

MULTI-MAGNON LUMINESCENCE SIDEBANDS IN
ANTIFERROMAGNETS

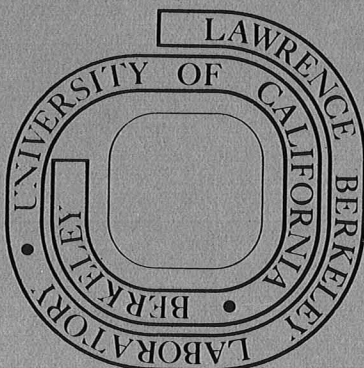
T. C. Chiang, P. Salvi, J. Davies, and
Y. R. Shen

December 1977

Prepared for the U. S. Department of Energy
under Contract W-7405-ENG-48

For Reference

Not to be taken from this room



LBL-6992
C-1

LEGAL NOTICE

This report was prepared as an account of work sponsored by the United States Government. Neither the United States nor the Department of Energy, nor any of their employees, nor any of their contractors, subcontractors, or their employees, makes any warranty, express or implied, or assumes any legal liability or responsibility for the accuracy, completeness or usefulness of any information, apparatus, product or process disclosed, or represents that its use would not infringe privately owned rights.

MULTI-MAGNON LUMINESCENCE SIDEBANDS
IN ANTIFERROMAGNETS

T. C. Chiang, P. Salvi,[†] J. Davies,[‡] and Y. R. Shen

DECEMBER 1977

Prepared for the U. S. Energy Research and
Development Administration under Contract W-7405-ENG-48

[†]Permanent address: Istituto di Chimica Fisica, Via G. Capponi 9,
50121 Firenze, ITALY

[‡]Permanent address: Physics Department, University College of Swansea,
Singleton Park Swansea SA2 8PP, GREAT BRITAIN

Submitted to Physical Review Letters

LBL-6992

MULTI-MAGNON LUMINESCENCE SIDEBANDS
IN ANTIFERROMAGNETS

T. C. Chiang, P. Salvi,[†] J. Davies,[‡] and Y. R. Shen

Department of Physics, University of California
Berkeley, California 94720

and

Materials and Molecular Research Division
Lawrence Berkeley Lab, Berkeley, California

DECEMBER 1977

ABSTRACT

Using pulsed excitation and detection, we have observed multi-magnon (≤ 7) luminescence sidebands of the ${}^4T_{1g}({}^4G) \rightarrow {}^6A_{1g}({}^6S)$ excitonic transition in MnF_2 , $KMnF_3$, and $RbMnF_3$. A simple model is proposed to explain the results qualitatively.

[†]Permanent address: Istituto di Chimica Fisica, Via G. Capponi 9,
50121 Firenze, ITALY

[‡]Permanent address: Physics Department, University College of Swansea,
Singleton Park Swansea SA2 8PP, GREAT BRITAIN

Magnon sidebands associated with excitonic absorption and emission in antiferromagnetic systems have long been a subject of extensive theoretical and experimental studies.^{1,2} Among the many antiferromagnets, the fluorides, MnF_2 in particular, have been most thoroughly investigated.³⁻⁵ Yet work is often limited to one- and two-magnon sidebands. Higher-order magnon sidebands are difficult to observe because they are either too weak or buried in the background. In the luminescence spectrum, strong background usually arises from impurity emission bands.⁶ With pulsed excitation and detection, however, long-lived impurity luminescence can be largely suppressed. This letter reports our recent observation of luminescence spectra of up to 7-magnon sidebands in MnF_2 and a few less in KMnF_3 and RbMnF_3 using such a technique. We interpret the results qualitatively by a simple two-ion local interaction model. Multi-magnon sidebands have earlier been predicted by Bhandari and Falicov from the sudden approximation model.⁷ In KMnF_3 , n-magnon sidebands with $n \leq 3$ have been observed by Strauss et al.,⁸ but no theoretical interpretation of the results has been attempted.

In our experiment, the samples were immersed in superfluid liquid helium. A tunable flash-pumped dye laser was used as the excitation source. The laser pulses had a pulsewidth of 0.4 μsec and an energy of a few millijoules per pulse. Luminescence from a sample was collected with either 90° or backward scattering geometry depending on the sample dimensions and was analyzed by a double monochromator followed by a photomultiplier and a gated PAR-162 boxcar integrator. The gate with an adjustable width (1 - 20 μsec) was triggered by the exciting laser pulse which was simultaneously monitored for signal normalization. To eliminate possible

pickup, gate opening was delayed by 1 μ sec after the leading edge of the laser pulse.

Since the impurity luminescence in the crystals we were interested in had rather long lifetimes (> 1 msec) we could eliminate most of it by using a relatively short gate width ($\lesssim 20$ μ sec). The laser pulse repetition rate was also kept low (≤ 6 pps) in order to suppress the exceptionally long-lived impurity lines. Then the spectrum obtained was believed to be essentially intrinsic. This is supported by the following experimental observations. (1) With increasing gate width, impurity luminescence lines showed up with increasing strength. (2) For different samples with different impurity luminescence, the intrinsic luminescence spectrum was the same. (3) The intrinsic luminescence at low excitation intensity normalized by photons absorbed was independent of the exciting laser wavelength λ_0 , while the impurity luminescence intensity changed rapidly with varying λ_0 . (4) Intrinsic luminescence depended strongly on the excitation intensity. In MnF_2 for example, the intrinsic luminescence lifetime decreased from ~ 200 μ sec at low excitation intensities to ~ 5 μ sec at ~ 50 MW/cm^2 . At high excitation intensities, the luminescence decay became more and more non-exponential with a very steep initial slope (presumably due to exciton-exciton collisions), and the luminescence intensity was no longer proportional to the excitation intensity.

Figure 1 shows the typical polarized intrinsic luminescence spectra of MnF_2 we have obtained. Conventional notations σ , α , and π are used to denote the three polarization geometries ($\vec{E} \perp \hat{c}$, $\vec{k} \perp \hat{c}$), ($\vec{E} \perp \hat{c}$, $\vec{k} \parallel \hat{c}$), and ($\vec{E} \parallel \hat{c}$, $\vec{k} \perp \hat{c}$) respectively. Lines E_1 and E_2 are the well-known exciton lines due to magnetic dipole transitions within the ${}^4T_{1g} \longrightarrow {}^6A_{1g}$

manifold. Sharp bands σ_1 and π_1 are the electric-dipole-allowed one-magnon sidebands of E_1 . The π_1 sideband is relatively weak, and so far as we know, its observation has never been reported in the literature. We have found that just like the σ_1 emission,³ the π_1 emission can be very well described by the theory of Loudon² with no need of invoking exciton-magnon interaction. The antiStokes emission of σ_1 and π_1 is also evident in Fig. 1. From the theoretical fit of the π_1 Stokes and anti-Stokes emission,⁹ we have deduced an effective crystal temperature of 13.8° K which agrees well with that obtained from the strength ratio of E_1 and E_2 .

Figure 1 also shows a series of luminescence peaks at lower energies. They form a more or less regular progression. Neighboring peaks are separated by $\sim 55 \text{ cm}^{-1}$ which is the maximum magnon frequency in MnF_2 .¹⁰ They are therefore identified as the multi-magnon sidebands. Arrows in Fig. 1 indicate where the cutoff frequencies of the multi-magnon sidebands should be. The polarization properties suggest that these sidebands are of electric-dipole origin. The π -polarization spectrum is however significantly different from the σ - and α -polarization spectra. With increasing temperature, the multi-magnon sidebands as well as the one-magnon sidebands gradually smeared out into the background as they should. As shown in Fig. 1, up to 7-magnon sidebands were actually observed in MnF_2 . Higher-order magnon sidebands might exist, but our spectra were terminated by the difficulty of positively identifying small structure on the rising background. Phonon-assisted optical transitions are presumably responsible for this strong luminescence background.

We have observed similar multi-magnon sidebands in the luminescence

spectra of KMnF_3 and RbMnF_3 as shown in Fig. 2. As is well-known, the exciton and magnon structures of these crystals closely resemble those of MnF_2 .¹¹ In KMnF_3 , sidebands up to 5 magnons show up clearly. They are regularly spaced with a frequency separation close to the maximum magnon frequency¹² of 76.3 cm^{-1} . In RbMnF_3 , the E_2 exciton line is too weak to be observed. Also, under our experimental conditions, two impurity lines at 5493 \AA and 5517 \AA still remained visible although they were greatly reduced in strength. As shown in Fig. 2, we have observed up to 3-magnon sidebands associated with E_1 in RbMnF_3 . They are almost regularly spaced by the maximum magnon frequency¹³ of 71 cm^{-1} . Interesting enough, we have also observed an almost identical series of magnon sidebands associated with the impurity exciton at 5493 \AA . This strongly suggests the localized nature of the phenomenon.

We now concentrate our theoretical interpretation of the results on MnF_2 . The discussion is equally applicable to KMnF_3 and RbMnF_3 . Fig. 3(a) shows schematically the dispersions of magnons and E_1 and E_2 excitons in MnF_2 . An E_1 exciton with wave vector \vec{k} can recombine by emitting simultaneously a magnon at \vec{k} and a photon. This gives rise to the one-magnon sideband.³ It is of course possible for an exciton to emit several magnons and a photon in the recombination. From the perturbation point of view, such a process would appear to be of higher order. This is certainly not true for the observed multi-magnon sidebands since the luminescence peaks in Fig. 1 are generally of comparable magnitude. We can however qualitatively explain the results by the following two-ion local interaction model.

Figure 3(b) shows the energy level diagrams of three neighboring Mn

ions;⁴ A and B are nearest neighbors on the same sublattice while A and C are second nearest neighbors on the opposite sublattices. The ground states $\langle g, m_s |$ of each ion are split by the exchange field into 6 Zeeman sublevels denoted by the spin quantum number $m_s = \pm 5/2, \pm 3/2, \text{ and } \pm 1/2$. The excited state E_1 is a mixed state $\sum_{m'_s} a_{m'_s} \langle e, m'_s |$ with $m'_s = \pm 1/2, \pm 3/2$, although $\langle e, m'_s = 3/2 |$ or $\langle e, m'_s = -3/2 |$ may dominate. In addition to the exchange field, there is also the off-diagonal exchange interaction $J_{ij} S_i^{\pm} S_j^{\mp}$ between ion pairs. We shall treat it as a perturbation. Then, if the Mn ion A is initially excited, the one-magnon sideband emission results from an allowed electronic transition $\langle e, m'_s |_A \rightarrow \langle e', 3/2 |_A$ followed by an exchange spin-flip transition between A and B, $\langle e', 3/2 |_A \langle g, 5/2 |_B \rightarrow \langle g, 5/2 |_A \langle g, 3/2 |_B$, or from the exchange spin-flip $\langle e, m'_s |_A \langle g, 5/2 |_B \rightarrow \langle e', 5/2 |_A \langle g, 3/2 |_B$ followed by the allowed transition $\langle e', 5/2 |_A \rightarrow \langle g, 5/2 |_A$. Either process involves $\Delta m_s = 1$ corresponding to the emission of one magnon. Now, similar physical processes of the same perturbation order can give rise to the n-magnon sidebands with $n \leq 6$. For example, $\langle e, m'_s |_A \rightarrow \langle e', 3/2 |_A$ followed by $\langle e', 3/2 |_A \langle g, -5/2 |_C \rightarrow \langle g, 1/2 |_A \langle g, -3/2 |_C$ via $J_{AC} S_A^- S_C^+$ leads to a 3-magnon sideband which can have comparable strength to the one-magnon sideband. Experimentally, the π -polarization spectrum in Fig. 1 even shows a 3-magnon sideband stronger than the one-magnon sideband. In a similar manner, the 2-magnon sideband can be explained by $\langle e, m'_s |_A \rightarrow \langle e', 1/2 |_A$ followed by $\langle e', 1/2 |_A \langle g, 5/2 |_B \rightarrow \langle g, 3/2 |_A \langle g, 3/2 |_B$ and others; the 4-magnon sideband can be explained by $\langle e, m'_s |_A \rightarrow \langle e', 1/2 |_A$ followed by $\langle e', 1/2 |_A \langle g, -5/2 |_C \rightarrow \langle g, -1/2 |_A \langle g, -3/2 |_C$ and others; etc.

In this model with $J_{ij} S_i^{\pm} S_j^{\mp}$ treated as a perturbation, the n-magnon sidebands with $n > 6$ will have to arise from a higher-order process utiliz-

ing $J_{ij} S_i^+ S_j^-$ more than once. Strictly speaking, we should treat the exchange interaction as a strong coupling Hamiltonian and solve the eigenenergies and eigenstates for a cluster of neighboring Mn ions. If the spin part is isolated from the orbital part, then this is just the sudden approximation model proposed by Bhandari and Falicov.⁷ In such a model, all the multi-magnon sidebands are treated on the same footing.

It is not easy to be quantitative in the above discussion. A realistic calculation taking into account just the nearest and next-nearest neighbor interactions is already extremely difficult. In addition, the relative amount of m'_s spin mixture in the excited state is not known so that the relative strengths of the magnon sidebands cannot be estimated. The magnon dispersion which results from exchange interaction between many ion pairs over a distance is not included in our model, and hence the spectral lineshape of these sidebands cannot be calculated. Nevertheless, the model does give a correct qualitative interpretation of the results. In particular, it explains how several multi-magnon luminescence sidebands can exist with comparable strengths. Our model treating the exchange interaction as a perturbation will predict in the first-order approximation only a one-magnon sideband in the absorption spectrum. It therefore also explains why n-magnon sidebands with $n > 2$ has never been observed.

We would like to thank Prof. L. Falicov for helpful discussions and Prof. W. D. Knight for providing us some of the crystals. This work was supported by the Division of Basic Energy Sciences, U.S. Department of Energy.

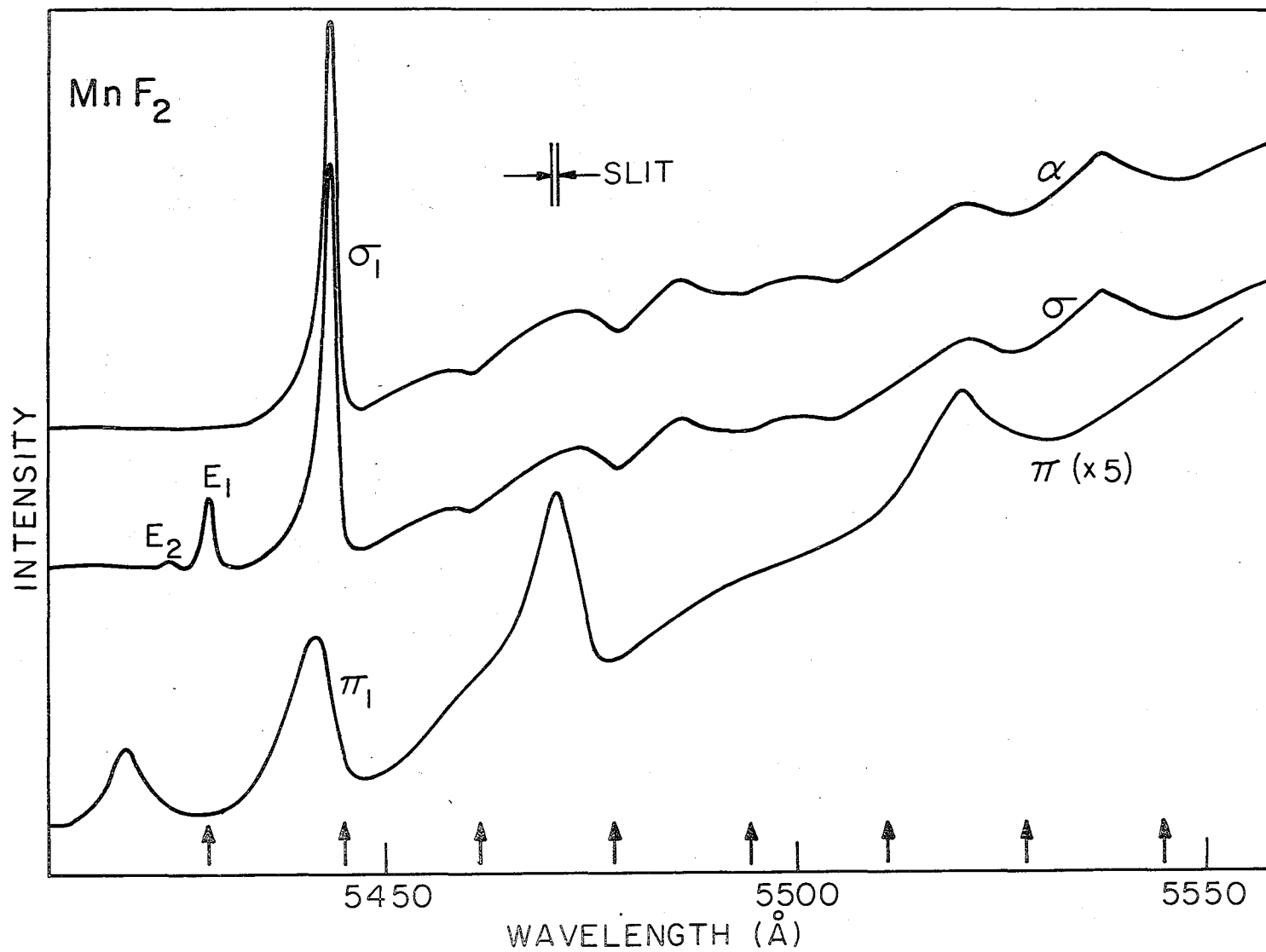
REFERENCES

1. See, for example, D. D. Sell, J. Appl. Phys. 39, 1030 (1968).
2. See, for example, R. Loudon, Advan. Phys. 17, 243 (1968).
3. R. E. Dietz, A. E. Meixner, H. J. Guggenheim, and A. Missetich, J. Luminesc. 1, 2, 279 (1970).
4. D. D. Sell, R. L. Greene, and R. M. White, Phys. Rev. 158, 489 (1967).
5. Y. Tanabe, K-I. Gondaira, and H. Murata, J. Phys. Soc. Japan 25, 1562 (1968).
6. R. L. Greene, D. D. Sell, R. S. Feigelson, G. F. Imbusch, and H. J. Guggenheim, Phys. Rev. 171, 600 (1968).
7. R. Bhandari and L. M. Falicov, J. Phys. C: Solid St. Phys. 5, 1445 (1972).
8. E. Strauss, V. Gerhardt, and H. Riederer, J. Luminesc. 12, 13, 239 (1976).
9. Further details will be published elsewhere.
10. A. Okazaki, K. C. Tuberfield, and R. W. H. Stevenson, Phys. Lett. 8, 9 (1964).
11. G. F. Imbusch and H. J. Guggenheim, Phys. Lett. 26A, 625 (1968); K. Aoyagi, J. Phys. Soc. Japan 22, 1516 (1967).
12. C. G. Windsor and R. W. H. Stevenson, Proc. Phys. Soc. 87, 501 (1966).
13. S. J. Pickart, M. F. Collins, and C. G. Windsor, J. Appl. Phys. 37, 1054 (1966).

FIGURE CAPTIONS

- Fig. 1 Polarized intrinsic luminescence spectra of MnF_2 . Laser intensity was $\sim 20 \text{ MW/cm}^2$ for the α - and σ -polarizations and $\sim 30 \text{ MW/cm}^2$ for the π -polarization; laser wavelength $\lambda_\ell = 5200 \text{ \AA}$; laser repetition rate = 6 pps; boxcar gate width = 1 μsec . Arrows indicate the theoretical cutoff points of the multi-magnon sidebands as explained in the text.
- Fig. 2 (a) Unpolarized intrinsic luminescence spectrum of KMnF_3 obtained with laser wavelength $\lambda_\ell = 5130 \text{ \AA}$, boxcar gate width = 10 μsec , laser repetition rate = 6 pps, and laser intensity = 4 MW/cm^2 . Arrows indicate the theoretical cutoff points of the multi-magnon sidebands.
- (b) Unpolarized luminescence spectrum of RbMnF_3 obtained with $\lambda_\ell = 5230 \text{ \AA}$, boxcar gate width = 1 μsec , laser repetition rate = 4 pps, and laser intensity = 60 MW/cm^2 . Features marked I are due to impurities. Long arrows indicate the intrinsic multi-magnon progression, while short arrows indicate the extrinsic multi-magnon progression starting from the impurity exciton at 5492.7 \AA .
- Fig. 3 (a) Schematic dispersion curves of excitons and magnons in MnF_2 .
- (b) Energy level diagrams of three neighboring Mn ions in the molecular field approximation. Ions A and B are on the same sublattice; the associated E_1 exciton state $\langle e, m'_s |$ may have a dominant $m'_s = 3/2$ component. Ion C is on the opposite sublattice; the associated E_1 exciton state $\langle e, m'_s |$ may have a dominant $m'_s =$

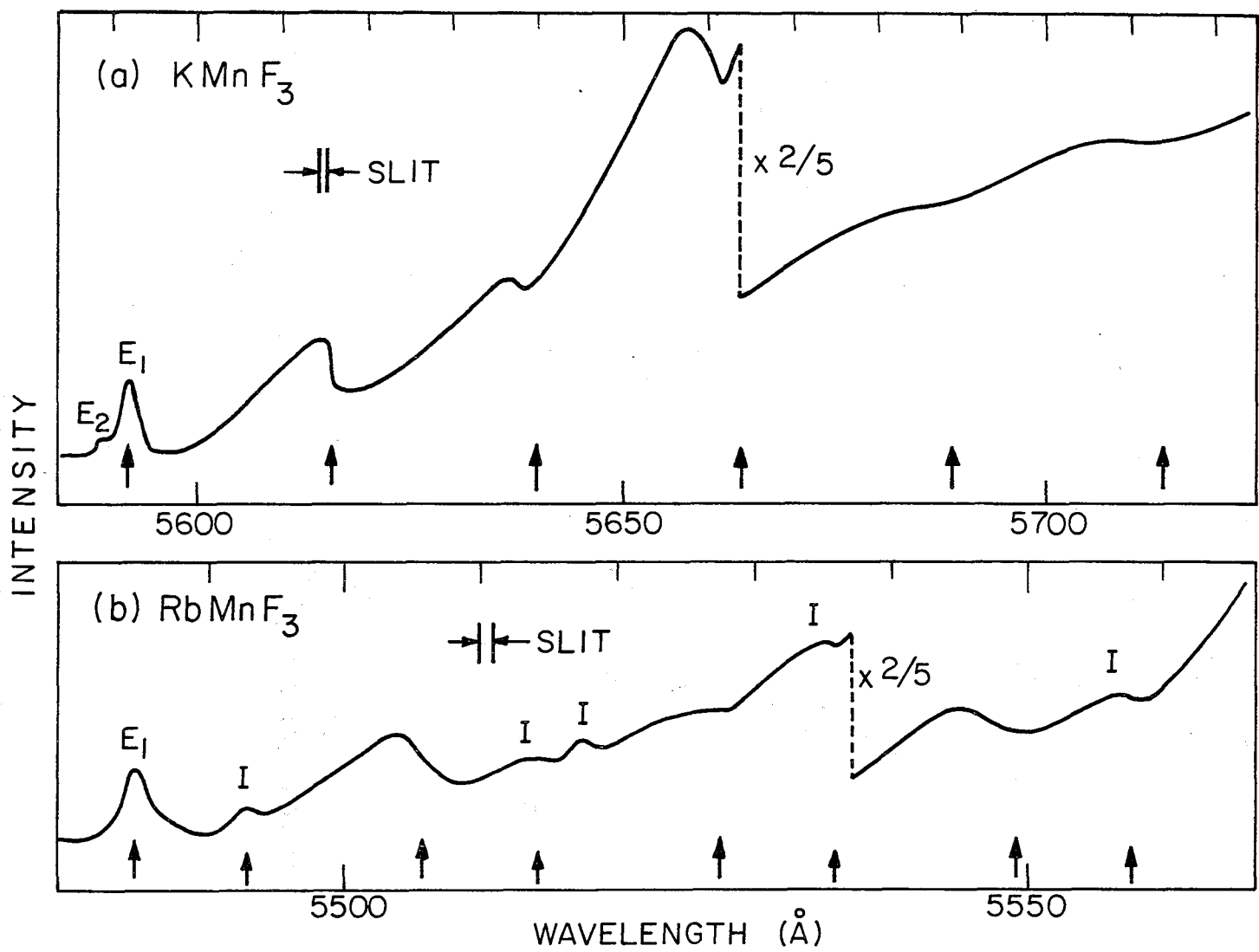
- 3/2 component. Transitions between $\langle e, m'_s |$ and $\langle g, m_s |$ are magnetic-dipole allowed.



XBL7712-6587

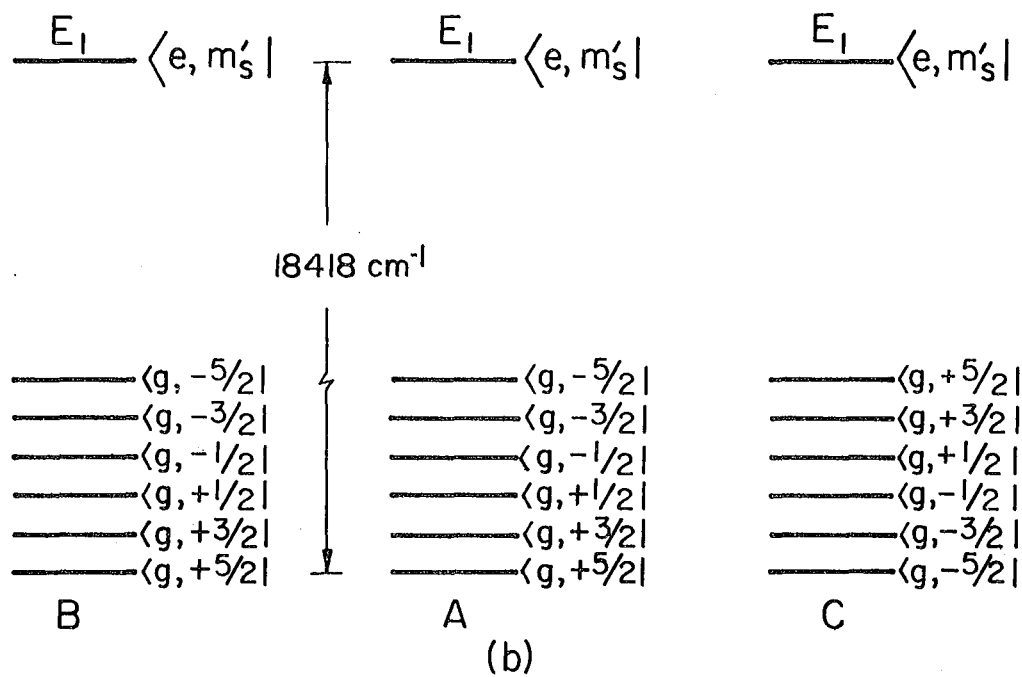
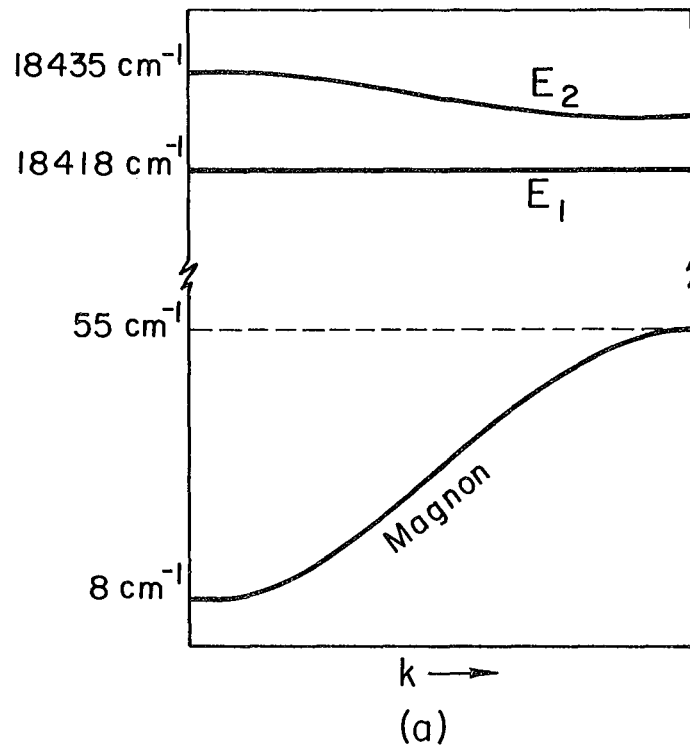
Fig. 1

0 9 9 0 0 4 4 0 0 6 5 0



XBL 7712-6588

Fig. 2



XBL7712-6586

Fig. 3



This report was done with support from the United States Energy Research and Development Administration. Any conclusions or opinions expressed in this report represent solely those of the author(s) and not necessarily those of The Regents of the University of California, the Lawrence Berkeley Laboratory or the United States Energy Research and Development Administration.